Palm Cove, Queensland, Australia

13 – 18 July 2003

# Laser Spectroscopy

Proceedings of the XVI International Conference


editors

Peter Hannaford
Andrei Sidorov

Swinburne University of Technology, Australia

Hans Bachor
Ken Baldwin

Australian National University



World Scientific

NEW JERSEY • LONDON • SINGAPORE • SHANGHAI • HONG KONG • TAIPEI • CHENNAI

*Published by*

World Scientific Publishing Co. Pte. Ltd.

5 Toh Tuck Link, Singapore 596224

*USA office:* Suite 202, 1060 Main Street, River Edge, NJ 07661

*UK office:* 57 Shelton Street, Covent Garden, London WC2H 9HE

**British Library Cataloguing-in-Publication Data**
A catalogue record for this book is available from the British Library.

**LASER SPECTROSCOPY**
**Proceedings of the XVI International Conference**



ISBN 981-238-616-5

Printed in Singapore.

# ULTRA-PRECISE PHASE CONTROL OF SHORT PULSES – APPLICATIONS TO NONLINEAR SPECTROSCOPY*

YUN YE, LISENG CHEN, R. JASON JONES,
KEVIN HOLMAN AND DAVID J. JONES
*JILA, National Institute of Standards and Technology and University of Colorado*
*Boulder, Colorado 80309-0440, USA*
*E-mail: Ye@JILA.colorado.edu*

Recent progress in precision control of pulse repetition rate and carrier-envelope phase of ultrafast lasers has found a wide range of applications in both precision spectroscopy and ultrafast science. In this contribution we discuss the impact of optical frequency comb to precision molecular spectroscopy, optical standards, nonlinear optics, and sensitive detection.

## 1. Introduction

Precise phase control of femtosecond lasers has become increasingly important as novel applications utilizing the femtosecond laser-based optical comb are developed that require greater levels of precision and higher degrees of control.[1] Improved stability is beneficial for both "frequency domain" applications, where the relative phase or "chirp" between comb components is unimportant (e.g., optical frequency metrology), and, perhaps more importantly, "time domain" applications where the pulse shape and/or duration is vital, such as in nonlinear optical interactions.[2] For both types of applications, minimizing jitter in the pulse train and noise in the carrier-envelope phase is often critical to achieve the desired level of precision. Phase-stabilized mode-locked femtosecond lasers have played a key role in recent advances in optical frequency measurement,[3,4] carrier-envelope phase stabilization,[2,5,6] all-optical atomic clocks,[7,8] optical frequency synthesizers,[9] coherent pulse synthesis,[10] and ultra-broad, phase coherent spectral generation.[11]

The capability of absolute optical frequency measurements in the visible and IR spectral regions adds a new meaning to the term of precision molecular spectroscopy. Understanding of molecular structure and dynamics often involves detailed spectral analysis over a broad wavelength range. Such a task can now be accomplished with a desired level of accuracy uniformly across all relevant spectral windows, allowing precise investigations of minute changes in the

* This work is supported by ONR, NASA, NIST and NSF.

molecular structure over a large dynamic range. For example, absolute frequency measurement of vibration overtone transitions and other related resonances (such as hyperfine splitting) will reveal precise information about the molecular potential energy surface and relevant perturbation effects. We have pursued a similar study in iodine molecules, performing high-resolution and high-precision measurement of hyperfine interactions of the first excited electronic state ($B$) of $I_2$ over an extensive range of vibrational and rotational quantum numbers towards the dissociation limit. Experimental data demonstrate systematic variations in the hyperfine parameters that confirm calculations based on *ab initio* molecular potential energy curves and electronic wave functions derived from a separated-atomic basis set. We have accurately determined the state-dependent quantitative changes of hyperfine interactions caused by perturbations from other electronic states and identified the respective perturbing states. Our work in $I_2$ near the dissociation limit is also motivated by the desire to improve cell-based portable optical frequency standards.[12] Indeed, $I_2$-stabilized lasers have already demonstrated high stability ($< 5 \times 10^{-14}$ at 1 s averaging time) and have served well for optical atomic clocks.[8]

For the time domain applications to molecular spectroscopy, stabilization of the "absolute" carrier-envelope phase at a level of tens of milli-radians has been demonstrated and this phase coherence is maintained over an experimental period exceeding many minutes,[13] paving the groundwork for synthesizing electric fields with known amplitude and phase at optical frequencies. Working with two independent femtosecond lasers operating at different wavelength regions, we have synchronized the relative timing between the two pulse trains at the femtosecond level,[14] and also phase locked the two carrier frequencies, thus establishing phase coherence between the two lasers. By coherently stitching optical bandwidth together, a "synthesized" pulse has been generated.[10] With the same pair of Ti:sapphire mode-locked lasers, we have demonstrated widely tunable femtosecond pulse generation in the mid- and far- IR using difference-frequency-generation.[15] The flexibility of this new experimental approach is evidenced by the capability of rapid and programmable switching and modulation of the wavelength and amplitude of the generated IR pulse. A fully developed capability of producing phase-coherent visible and IR pulses over broad spectral bandwidths, coupled with arbitrary control in amplitude and pulse shape, represents the ultimate instrumentation for coherent control of molecular systems.

The simultaneous control of timing jitter (repetition rate) and carrier-envelope phase can be used to phase coherently superpose a collection of successive pulses from a mode-locked laser. For example, by stabilizing the two degrees of freedom of a pulse train to an optical cavity acting as a coherent delay, constructive interference of sequential pulses will be built up until a cavity dump is enabled to switch out the "amplified" pulse.[16] Such a passive pulse "amplifier", along with the synchronization technique we developed for pulse

synthesis, has made a strong impact on the field of nonlinear-optics based spectroscopy and imaging of bio-molecular systems, showing significant improvements in experimental sensitivity and spatial resolution.[17,18] With the enhanced detection sensitivity comes the capability of tracking real time biological dynamics. An ultrafast laser locked to a high stability cavity is also expected to demonstrate extremely low pulse jitter and carrier-envelope phase noise, which will be particularly attractive for time-domain experiments. In addition, we are exploring the use of pulse-cavity interactions to obtain highly sensitive intracavity spectroscopy (linear and non-linear) with a wide spectral coverage, as well as to enhance nonlinear interaction strengths for high efficiency nonlinear optical experiments.

## 2. $I_2$ Hyperfine Interactions, Optical Frequency Standards and Clocks

The hyperfine structure of $I_2$ rovibrational levels includes four contributions: nuclear electric quadrupole ($eqQ$), spin-rotation ($C$), tensorial spin-spin ($d$), and scalar spin-spin ($\delta$) interactions. Agreement between experiment and theory using the four-term effective Hamiltonian is at the kilohertz level for a few selected transitions. For the first excited electronic state $B$ with the $^2P_{3/2} + {}^2P_{1/2}$ dissociation limit, our goal is to perform a systematic high-precision investigation of hyperfine interactions over an extensive range of rovibrational quantum numbers coupled with a large range of internuclear separations. Such a study has allowed us to understand the rovibrational dependence of the hyperfine interactions (as well as the dependence on internuclear distance) based on *ab initio* molecular potential energy curves and the associated electronic wave functions. Careful analysis of various perturbation effects leads to precise determination of molecular structure over a large dynamic range.

Prior studies have concentrated on a few isolated rovibrational levels for the high vibrational states $v' = 40$ to 82 in the $B$ state.[19] For vibrational levels below $v' = 43$, only functional forms on the state-dependent variations of the hyperfine interactions have been investigated from empirical data.[20] Combining absolute optical frequency metrology with high-resolution and broad wavelength-coverage laser spectroscopy, we have measured ~ 80 rovibrational transitions with the upper vibrational levels (from $v' = 42$ up to $v' = 70$) stretching from a closely bonded molecular basis to a separated-atomic basis appropriate for the $^2P_{3/2} + {}^2P_{1/2}$ dissociation limit, providing kHz-level line accuracies for most hyperfine components. Figure 1 illustrates systematic rovibrational dependences for all four hyperfine parameters. Each solid line is a fit of experimental data for rotational dependence belonging to a single vibrational ($v'$) level. In general, all hyperfine parameters have monotonic dependence on both rotational and vibrational quantum numbers except for the levels in the vicinity of $v' = 57$ to 59. However, the $v$-dependence of $eqQ_B$ reverses its trend after $v' = 60$. For the

sake of figure clarity, the $eqQ_B$ data for $v' > 60$ are not shown. Another important observation is that for levels of $v' = 57 - 59$ all hyperfine parameters except for $C_B$ bear abnormal $J$-dependences due to perturbations from a $^1g$ state through accidental rotational resonances.

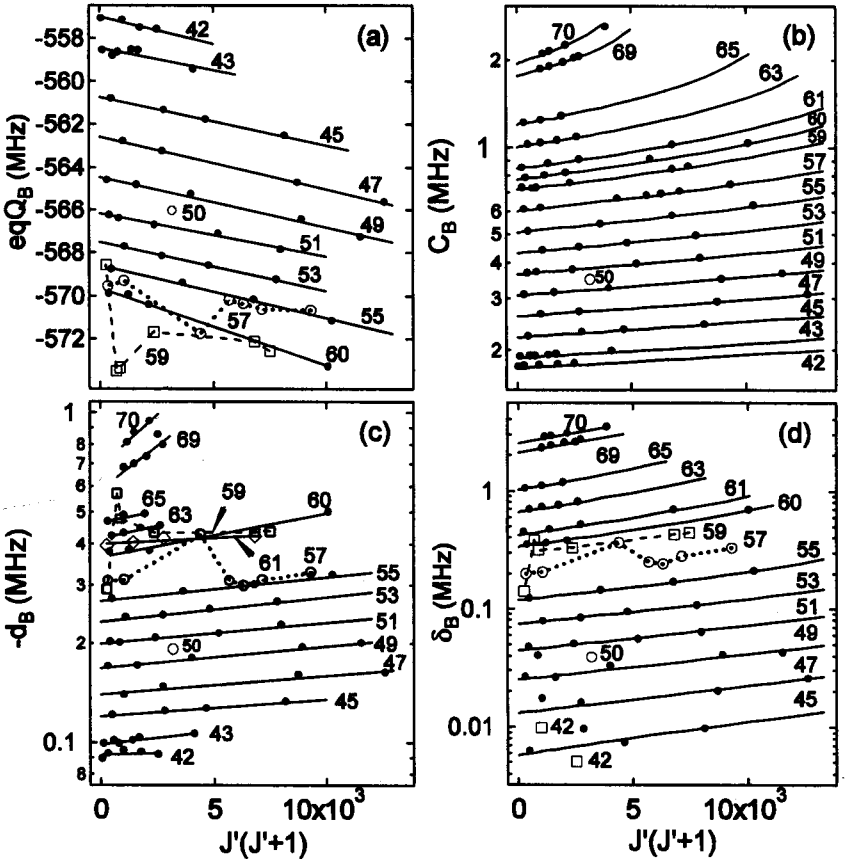


Figure 1. Rovibrational dependence of the $B$ state hyperfine parameters (a) $eqQ_B$, (b) $C_B$, (c) $d_B$, and (d) $\delta_B$. Note (b), (c), and (d) are semilog plots and the vertical scale of (c) has been inverted. Each solid line is the $J$-dependence for each vibrational level ($v'$ indicated in the figure). Experimental data in squares and open circles show abnormal variations of $eqQ_B$, $d_B$, and $\delta_B$ around $v' = 57$ and 59.

Combining data from this work and from the literature,[20] investigations of the hyperfine spectra now cover the majority of the vibrational levels ($3 \le v' \le 82$) in the $B$ state. Therefore, it is now possible and useful to explore the global trend of these hyperfine parameters in the $B$ state. Suppressing the rotational dependence, hyperfine parameters as functions of pure vibrational energy $E(v')$ are found to increase rapidly when molecules approach the dissociation limit,

which is a result of the increasingly strong perturbations from other high-lying electronic states sharing the same dissociation limit with $B$. While $C_B$'s variation is smooth over the whole range, $eqQ_B$, $d_B$, and $\delta_B$ all have local irregularities at three positions: $v' = 5$ where the $B'':1_u$ state crosses nearby, around $v' = 57$ to 59 (see discussions above), and from $v' = 76$ to 78, due to the $1_g$ state.[19]

To examine these hyperfine parameters in terms of internuclear separation $R$, the vibrational average of the hyperfine parameters is removed by inverting the expression $O(v',J') = \langle v'J'|O(R)|v'J'\rangle$, where $O(v',J')$ denotes one of the four hyperfine parameters. Consistent with $C_B$'s smooth variation, the interpolation function $C_B(R)$ has small residual errors (within ±0.02, relative) for the entire range from $v' = 3$ to 70. On the contrary, the large residual errors in the interpolation of $eqQ_B$, $d_B$, and $\delta_B$ for $v' \geq 56$ reflect their abnormal variations observed around $v' = 57$ and 59, restricting a reliable interpolation only to levels of $v' < 56$. In the region of $R < 5$ Å, valuable information can be readily extracted from $eqQ_B$ to assist investigation of $I_2$'s electronic structure. Unlike the other three hyperfine parameters whose major parts originate from perturbations at nearly all possible values of $R$, a significant part of $eqQ_B$ is due to the interaction between the nuclear quadrupole moment ($Q$) and the local electric field gradient ($q$(R)) generated by the surrounding charge distribution of a largely $B$ state character. Thus, for $R < 5$ Å, where perturbations from other electronic states are negligible, the vibration-removed interpolation function $eqQ_B(R)$, coupled with *a priori* information on $q(R)$, can be used to determine $I_2$ nuclear quadrupole moment or serve as a benchmark for molecular *ab initio* calculations of the electronic structure at various values of $R$.

Precision measurements on $B$-$X$ hyperfine spectra provide an alternative and yet effective way to investigate the potential energy curves (PECs) sharing the same dissociation limit with the $B$ state as well as the associated electronic wave functions. To demonstrate this, we perform calculations of $eqQ_B$, $C_B$, $d_B$, and $\delta_B$ based on the available PECs and electronic wave functions derived from a separated-atomic basis set. For both vibrational and rotational dependences, the *ab initio* calculation results agree very well with the experimental data for $v' \geq 42$ ($R$-centroid ≥ 3.9 Å). In short, we have extended the range of separated-atomic basis calculations from levels near the dissociation limit to low vibrational levels ($v' = 5$) and have found very good agreement with the experimental data on both vibrational and rotational dependences.

Besides these interesting studies in hyperfine structure, the narrow-linewidth $I_2$ transitions in this wavelength range also provide excellent cell-based optical frequency references for laser stabilization. Frequency-doubled Nd:YAG/$^{127}I_2$ at 532 nm has been proved to be one of the best portable optical frequency standards with compact size, reliability, and high stability ($< 5 \times 10^{-14}$ at 1 s). To reach a higher frequency stability, it is useful to explore $I_2$ transitions at wavelengths below 532 nm, where the natural linewidths decrease at a faster rate

than that for the line strengths. We have measured the systematic variation of the $I_2$ transition linewidths within the range of 532 - 498 nm, with the linewidth decreasing by nearly 6 times when the wavelength is changed from 532 nm to near the dissociation limit.[12] The high *S/N* results indicate that $I_2$ transitions in the wavelength range of 532 - 501 nm hold great promise for future development of optical frequency standards, especially with the advent of all solid state Yb:YAG lasers. One exciting candidate is the 514.67 nm standard,[21] with a projected stability $< 1 \times 10^{-14}$ at 1 s. The $I_2$-based optical standard has been used to stabilize an entire octave-bandwidth spanning optical frequency comb based on a mode-locked Ti:sapphire laser, thus establishing an optical atomic clock where the RF signal is phase coherently derived from the $I_2$ optical transition.[8] With a coherent link established between the femtosecond Ti:sapphire laser and 1550-nm mode-locked laser sources,[22] precise time and frequency information can be transferred and disseminated from an optical atomic clock to remote sites via optical telecommunication networks.

## 3. Femtosecond Lasers and External Optical Cavities

Understanding the intricate interactions between ultra-short pulses and external passive optical cavities, along with subsequent development of capabilities to efficiently couple and coherently store ultra-short pulses of light inside a high finesse optical cavity, will open doors for a variety of exciting experiments. An immediate impact is on precision stabilization of ultrafast lasers.[23] Similar to the state-of-art stabilization of CW lasers, a cavity-stabilized ultrafast laser is expected to demonstrate superior short-term stability of both the pulse repetition frequency and the carrier-envelope phase. The improved stability is beneficial in particular for time-domain applications where the signal processing bandwidth is necessarily large. Another attractive application lies in broadband and ultrasensitive spectroscopy. The use of high finesse cavities has played a decisive role for enhancing sensitivity and precision in atomic and molecular spectroscopy. We expect a dramatic advancement in the efficiency of intracavity spectroscopy by exploiting the application of ultra-short pulses. In other words, a high detection sensitivity is achievable across the broad spectrum of the pulse simultaneously. Cavity-stabilization techniques for femtosecond lasers allow the comb structure of the probe laser to be precisely matched to the resonance modes of an empty cavity, allowing efficient energy coupling for a spectroscopic probe. Molecular samples introduced inside the high finesse cavity will have a strong impact on the dispersive properties of the cavity. In fact it is this dispersion-related cavity-pulling effect that will aid our sensitive detection process when we analyze the light transmitted through the cavity. Preliminary data on spectrally resolved, time-domain ring down measurement for intracavity loss over the entire femtosecond laser bandwidth are already quite promising.

To develop sources for ultrafast nonlinear spectroscopy, a properly designed dispersion compensated cavity housing a nonlinear crystal will provide efficient nonlinear optical frequency conversion of ultrashort optical pulses at spectral regions where no active gain medium exists. Furthermore, by simultaneously locking two independent mode-locked lasers to the same optical cavity, efficient sum and/or difference frequency generation can be produced over a large range of wavelengths. Under a similar motivation, a passive cavity can be used to explore coherent "amplification" of ultra short pulses, with cavity stabilization providing the means to phase coherently superpose a collection of successive pulses from a mode-locked laser. The coherently enhanced pulse stored in the cavity can be switched out using a cavity-dumping element (such as a Bragg cell), resulting in a single phase-coherent "amplified" pulse. The use of a passive cavity also offers the unique ability to effectively amplify pulses at spectral regions where no suitable gain medium exists, such as for the infrared pulses from difference-frequency mixing or the UV light from harmonic generation. Unlike actively dumped laser systems, the pulse energy is not limited by the saturation of a gain medium or a saturable absorber needed for mode-locking. Instead, the linear response of the passive cavity allows the pulse energy to build up inside the cavity until limited by cavity loss and/or dispersive pulse spreading. Therefore storage and amplification of ultra-short pulses in the femtosecond regime requires precise control of the reflected spectral phase of the resonator mirrors as well as the optical loss of the resonator. While the reflected phase and group delay of the mirrors only change the effective length of the resonator, the group delay dispersion (GDD) and higher-order derivatives of the group delay with respect to frequency affect the pulse shape. The net cavity GDD over the bandwidth of the pulse needs to be minimized in order to maintain the shape of the resonant pulse and allow for the coherent addition of energy from subsequent pulses.

We have applied the coherent pulse-stacking technique to both picosecond and femtosecond pulses. Initial studies have already demonstrated amplification of picosecond pulses of greater than 30 times at repetition rates of 253 kHz, yielding pulse energies greater than 150 nJ.[18] With significant room left for optimization of the cavity finesse (current value of ~ 350, limited by the cavity input-coupling mirror), we expect that amplifications greater than a hundred times are feasible, bringing pulse energies into the μJ range. While the use of picosecond pulses allows us to separate out complications arising from intra-cavity dispersion, for sub-100 femtosecond pulses, dispersive phase shifts in the cavity mirrors becomes an important topic. Preliminary results in enhancing low individual pulse energies for ~75 fs pulses illustrate the importance of GDD control. The external enhancement cavity incorporated specially designed negative GDD low-loss mirrors to simultaneously compensate for the Bragg cell's 3 mm of fused silica and provide a high finesse. The input coupling mirror transmission was ~ 0.8 %, with a measured cavity finesse of 440. An intracavity

energy buildup of 163 is expected, leading to single pulse amplifications of approximately 65 for the current setup given the 40% dumping efficiency of our Bragg cell. The negative GDD mirrors were designed to only partially compensate for the total cavity dispersion. The remaining cavity GDD was estimated at +20 to +30 $fs^2$. The excess dispersion results in pulse broadening and a non-uniform filtering of the transmitted pulse spectrum. Experimental results are in good agreement with independent numerical calculations. The observed amplification of only 18 times is therefore not surprising as the achievable pulse enhancement is limited by the lack of perfect resonance between the femtosecond comb and the external cavity. Controlling the intracavity pressure will allow fine tuning of the net cavity GDD to zero.

We thank E. Potma, X.-S. Xie, S. Foreman, I. Thoman, H. Kapteyn, S. Cundiff, T. Fortier, and E. Ippen for fruitful collaborations and J. L. Hall for his support and inspirations. K. Holman is a Hertz Foundation Graduate Fellow. R. J. Jones is a National Research Council Research Associate Fellow.

## References

1. S. T. Cundiff and J. Ye, *Rev. Modern Phys.* **75**, 325 (2003).
2. A. Baltuska et al., *Nature* **421**, 6923 (2003).
3. T. Udem et al., *Phys. Rev. Lett.* **82**, 3568 (1999).
4. J. Ye et al., *Phys. Rev. Lett.* **85**, 3797 (2000).
5. D. J. Jones et al., *Science* **288**, 635 (2000).
6. A. Apolonski et al., *Phys. Rev. Lett.* **85**, 740 (2000).
7. S. A. Diddams et al., *Science* **293**, 825 (2001).
8. J. Ye, L.-S. Ma and J. L. Hall, *Phys. Rev. Lett.* **87**, 270801 (2001).
9. J. D. Jost, J. L. Hall and J. Ye, *Opt. Express* **10**, 515 (2002).
10. R. K. Shelton et al., *Science* **293**, 1286 (2001).
11. A. Baltuska, T. Fuji and T. Kobayashi, *Phys. Rev. Lett.* **88**, 133901 (2002).
12. W.-Y. Cheng et al., *Opt. Lett.* **27**, 571 (2002).
13. T. M. Fortier et al., *Opt. Lett.* **27**, 1436 (2002).
14. R. K. Shelton et al., *Opt. Lett.* **27**, 312 (2002).
15. S. Foreman, D. J. Jones and J. Ye, *Opt. Lett.* **28**, 370 (2003).
16. R. J. Jones and J. Ye, *Opt. Lett.* **27**, 1848 (2002).
17. E. Potma et al., *Opt. Lett.* **27**, 1168 (2002).
18. E. Potma et al., *Opt. Lett.* **28**, 1835 (2003).
19. J. Vigué, M. Broyer and J. C. Lehmann, *Phys. Rev. Lett.* **42**, 883 (1979).
20. B. Bodermann, H. Knöckel and E. Tiemann, *Eur. Phys. J. D* **19**, 31 (2002).
21. R. J. Jones et al., *Appl. Phys. B* **74**, 597 (2002).
22. K. W. Holman et al., *Opt. Lett.*, in press (2003).
23. R. J. Jones and J.-C. Diels, *Phys. Rev. Lett.* **86**, 3288 (2001).